



Spike trains in a stochastic Hodgkin–Huxley system

Henry C. Tuckwell*

Department of Mathematics, University of California San Diego, Gillman Drive, La Jolla, CA 92093, USA

Received 14 March 2004; accepted 24 September 2004

Abstract

We consider a standard Hodgkin–Huxley model neuron with a Gaussian white noise input current with drift parameter μ and variance parameter σ^2 . Partial differential equations of second order are obtained for the first two moments of the time taken to spike from (any) initial state, as functions of the initial values. The analytical theory for a 2-component (V, m) approximation is also considered. Let μ_c (≈ 4.15) be the critical value of μ for firing when noise is absent. Large sample simulation results are obtained for $\mu < \mu_c$ and $\mu > \mu_c$, for many values of σ between 0 and 25. For the time to spike, the 2-component approximation is accurate for all σ when $\mu = 10$, for $\sigma > 7$ when $\mu = 5$ and only when $\sigma > 15$ when $\mu = 2$. When $\mu < \mu_c$, σ must be large to induce firing so paths are always erratic. As the noise increases, the coefficient of variation (CV) has a well-defined minimum, and then climbs steadily over the range considered. If μ is just above μ_c , when the noise is small, paths are close to deterministic and the standard deviation and CV of the time to spike are small. As σ increases, some very erratic paths (some almost oscillatory) appear, making the mean, standard deviation and CV of the spike time very large. These erratic paths start to have a large influence, so all three statistics have very pronounced maxima at intermediate σ . When $\mu \gg \mu_c$, most paths show similar behavior and the moments exhibit smoothly changing behavior as σ increases. Thus there are a different number of regimes depending on the magnitude of μ relative to μ_c : one when μ is small and when μ is large; but three when μ is close to and above μ_c . Both for the Hodgkin–Huxley (HH) system and the 2-component approximation, and regardless of the value of μ , the CV tends to about 1.3 at the largest value (25) of σ considered. We also discuss in detail the problem of determining the interspike interval and give an accurate method for estimating this random variable by decomposing the interval into stochastic and almost deterministic components.

© 2004 Elsevier Ireland Ltd. All rights reserved.

Keywords: Stochastic neuron model; Firing times; Hodgkin–Huxley

1. Introduction

There has been a continuing strong interest in the stochastic nature of neuronal spiking with regard to an

understanding of “information processing” (deCharms and Zador, 2000; Steinmetz et al., 2001; Manwani et al., 2002). Furthermore, there have been many experimental studies of the spike trains emitted by cortical cells in response to natural and artificial stimulation (Stein, 1967; Steriade et al., 1973; Burns and Webb, 1976; Kreiter and Singer, 1996; Chen et al., 1996) but it

E-mail addresses: htuckwel@math.ucsd.edu,
tuckwell@u444.jussieu.fr (H.C. Tuckwell).

* Tel.: +1 858 534 5863; fax: +1 858 452 9848.

is still uncertain which models reproduce experimental details (Troyer and Miller, 1998; Plesser and Gerstner, 2000). Various simplified models of cortical pyramidal cells have been investigated in an attempt to understand the role of the significant amounts of background activity (Destexhe and Pare, 2000; Meffin et al., 2004) in these cells. Such models include integrate and fire models with additive input or conductance-based input (Tuckwell, 1979) as well as fully non-linear models. Some recent studies try to characterize cellular activity in terms of five quantities—the mean output spike frequency, the CV of the interspike interval, the mean and variance of the (steady state) membrane potential and the effective membrane time constant (Meffin et al., 2004).

In this paper we address the problem of determining the firing times of a Hodgkin–Huxley neuron where the variability arises due to random synaptic input. This is distinguished from the effects of current fluctuations due to ion channel openings and closing (Skaugen and Walloe, 1979) and those studies where white noise is assumed in the equations for the variables h , m , and n (Fox and Lu, 1994; Schmid et al., 2004). Many mathematical approaches have been employed to solve this problem approximately by using simple models such as those involving an Ornstein–Uhlenbeck process (Gluss, 1967; Plesser and Gerstner, 2000), Fitzhugh–Nagumo system and the Hodgkin–Huxley (HH) system (Kistler et al., 1997; Tuckwell and Rodriguez, 1998; Feng and Li, 2001; Tuckwell et al., 2002). Some authors have made considerable progress in comparing analytical results for linearized versions to simulations of non-linear models for subthreshold steady state conditions (Steinmetz et al., 2000).

Early findings of significance were those of Yu and Lewis (1989) who found the frequency–current relation was linearized by noise. These authors also noted that the Hodgkin–Huxley model could provide a useful representation of the behaviour for certain mammalian central nervous system cells, but not at high (> 120 Hz) spike rates. Stochastic resonance was found in neuronal modeling and, with the advent of the greater availability of computing power, was investigated, for example, for an Hodgkin–Huxley system with an input current consisting of an Ornstein–Uhlenbeck process superimposed upon a sinusoidal term (Lee and Kim, 1999). More recently, Tiesinga et al. (2000), motivated in part by the problem of the irreproducibility of high coeffi-

cients of variation by simpler models, considered the statistics of spike trains produced by random input currents in HH models. These authors were able to distinguish the two regimes of current dominated and noise dominated firing.

Here we begin by outlining an analytical method of finding the statistics of the time to an action potential in the space-clamped stochastic Hodgkin–Huxley system by solving associated partial differential equations. The approach that we use can be employed for any conductance based model. Analytical methods of solution are pursued elsewhere (Tuckwell and Wan, 2004). Simulations are performed and analyzed for the stochastic differential equations for the HH model and its approximations. In the last part of the paper we address the problem of determining the interspike interval, which is a less tractable problem than characterizing the time to the first spike.

2. Theory

We consider the Hodgkin–Huxley equations (Hodgkin and Huxley, 1952) with additive Gaussian white noise current (Tuckwell, 1986, 1989) which is used to represent an approximation to Poisson trains of excitatory and inhibitory post-synaptic potentials

$$I_A(t) = \mu + \sigma \frac{dW}{dt}$$

with units $\mu\text{A}/\text{cm}^2$, W being a standard Wiener process. With such a current, the 4-component space-clamped system is

$$\begin{aligned} dV &= \frac{1}{C} \{ [\mu + \bar{g}_K n^4 (V_K - V) + \bar{g}_{Na} m^3 h (V_{Na} - V) \\ &\quad + g_1 (V_1 - V)] dt + \sigma dW \} \\ dn &= [\alpha_n (1 - n) - \beta_n n] dt \\ dm &= [\alpha_m (1 - m) - \beta_m m] dt \\ dh &= [\alpha_h (1 - h) - \beta_h h] dt, \end{aligned} \quad (1)$$

where C is the membrane capacitance in $\mu\text{F}/\text{cm}^2$, V is the depolarization from resting membrane potential in mV and V_K and V_{Na} are the Nernst equilibrium potentials (mV) for potassium and sodium ions. The constants \bar{g}_K and \bar{g}_{Na} are the maximal membrane conductances, in mS/cm^2 , for potassium and sodium. The dimensionless $[0, 1]$ -valued dynamical variables n , m , and h represent, respectively, the fractions of potas-

sium channel activation, sodium channel activation and sodium channel inactivation. The α - and β -coefficients are given in the Appendix A. The term $g_1(V_1 - V)$ is a current required to give a stable resting condition. Standard constants are as follows: $\bar{g}_K = 36$, $\bar{g}_{Na} = 120$, $g_1 = 0.3$, $V_K = -12$, $V_{Na} = 115$, $V_1 = 10.613$, $C = 1$.

Solution of the corresponding deterministic system, ($\sigma = 0$) using Runge–Kutta methods, reveals

$$-\frac{\partial p}{\partial \hat{t}} = \frac{\sigma^2}{2} \frac{\partial^2 p}{\partial \hat{v}^2} + \{c_1(V_K - \hat{v})\hat{x}^4 + c_2(V_{Na} - \hat{v})\hat{y}^3\hat{z} + c_3(V_1 - \hat{v}) + \mu\} \frac{\partial p}{\partial \hat{v}} + \{\alpha_n(\hat{v})(1 - \hat{x}) - \beta_n(\hat{v})\hat{x}\} \frac{\partial p}{\partial \hat{x}} \\ + \{\alpha_m(\hat{v})(1 - \hat{y}) - \beta_m(\hat{v})\hat{y}\} \frac{\partial p}{\partial \hat{y}} + \{\alpha_h(\hat{v})(1 - \hat{z}) - \beta_h(\hat{v})\hat{z}\} \frac{\partial p}{\partial \hat{z}},$$

(Stein, 1967; Rinzel, 1978) that there is a threshold current of about $\mu = 4.15$ required to elicit a single spike and that a sustained current of about $\mu = 6.5$ elicits a regular train of impulses. As μ increases, the spike frequency increases while the amplitude of the spikes decreases. We consider in this section the time to the appearance of a spike in (1) using first exit time theory for diffusion processes. In Section 4 we address the more complicated problem of determining the interspike interval.

In both the deterministic and stochastic cases, the waiting time for the first spike from the standard rest state $(V(0), n(0), m(0), h(0))$ is considerably less than the time interval between spikes as the system takes a while to settle into the regular (stochastic) firing mode. In the deterministic case, the trajectory of the phase point after the first spike is practically periodic but in the stochastic case there is considerable variability on each orbit, with greater variability occurring at sub-threshold values. Thus one distinguishes the random variable T_1 , the time to elicit the first spike, from resting conditions (although a different initial value could be chosen), from the subsequent interspike interval T (see further discussion in Section 4). For example, with $\mu = 20$ and $\sigma = 5$, the waiting time to the first spike from rest has a mean of about 1 ms whereas in the ensuing train, the mean interval between spikes 1 and 2 and subsequently is about 10 ms. For T_1 an initial condition, for example the rest state, is well defined. The characteristics of T_1 can be obtained experimentally by commencing with equilibrium conditions. In the mostly 1-component classical integrate and fire models, there is no distinction between the time to the first spike and the subsequent interspike interval.

Using our previous notation (Tuckwell, 1986), the backward Kolmogorov equation satisfied by the transition probability density function $p(v, x, y, z, t; \hat{v}, \hat{x}, \hat{y}, \hat{z}, \hat{t})$ of the four-dimensional process (V, X, Y, Z) , where X is the potassium activation variable n , Y is the sodium activation variable m , and Z is the sodium inactivation variable h , and where $\hat{v}, \hat{x}, \hat{y}, \hat{z}, \hat{t}$ are backward (earlier) variables, is

where $c_1 = \bar{g}_K/C$, $c_2 = \bar{g}_{Na}/C$ and $c_3 = g_1/C$. It is useful to define the differential operator \hat{L} so that this (linear) partial differential equation can be written

$$-\frac{\partial p}{\partial \hat{t}} = \hat{L}p.$$

If the initial value of (V, X, Y, Z) is $(\hat{v}, \hat{x}, \hat{y}, \hat{z})$ and this point lies in the four-dimensional set A then the n th moments $M_n(\hat{v}, \hat{x}, \hat{y}, \hat{z})$, $n = 0, 1, 2, \dots$, of the exit time of the four-dimensional process from A , are the solutions of the recursion system of partial differential equations

$$\hat{L}M_n = -nM_{n-1},$$

with boundary conditions that for $n \geq 1$, M_n vanish on the accessible boundaries of A and for $n = 0$, that $M_n = 1$ on the boundary of A .

When a spike is elicited from rest, the trajectory of the phase point prior to a spike entails major changes in the variables V and m (Y) but during the same epoch the variables n and h (X and Z) are often practically unchanged as will be seen in the next section. Under these conditions, but not during the interspike interval, a two-dimensional approximation to the Hodgkin–Huxley system is accurate. Then the values of n and h are held fixed at their initial values, denoted now by n_0 and h_0 , thus eliminating two differential equations. Hence we consider the process (\bar{V}, \bar{m}) as a 2-component approximation satisfying the equations

$$d\bar{V} = \frac{1}{C} \{ [\mu + \bar{g}_K n_0^4 (V_K - \bar{V}) + \bar{g}_{Na} m^3 h_0 (V_{Na} - \bar{V}) + g_1 (V_1 - \bar{V})] dt + \sigma dW \} \quad d\bar{m} = [\alpha_m (1 - \bar{m}) - \beta_m \bar{m}] dt.$$

We denote the time of first passage of the process $(\bar{V}, \bar{m}) = (\bar{V}, \bar{Y})$ with initial value (\hat{v}, \hat{y}) to (v_θ, y_θ) by $\bar{T}_1(\hat{v}, \hat{y}; v_\theta, y_\theta)$ with expected value $E(\bar{T}_1) = \bar{F}(\hat{v}, \hat{y}; v_\theta)$ and second moment $E(\bar{T}_1^2) = \bar{G}(\hat{v}, \hat{y}; v_\theta)$. The analytical approach to finding the moments in this 2-component approximation is given elsewhere (Tuckwell and Wan, 2004) some numerical results being mentioned below. In the 2-component approximation, there are no complete spikes only the rising phases of them, as there is no possibility of recovery.

3. Results for the time to the first spike

Even though the original HH system was based on the electrophysiology of squid axon, it has been found to be useful as a general non-linear model neuron (Yu and Lewis, 1989), being more realistic than the simplified Fitzhugh–Nagumo system. For applications beyond squid axon, the HH system has been modified by the addition of various conductances other than the standard potassium, sodium and leakage conductances (Mainen et al., 1995; Pare et al., 1998; Destexhe and Pare, 2000). In order to make the original HH model more relevant to cells which are important in information processing in the mammalian brain, we seek values of μ and σ which would give an approximate representation of the firing of cortical neurons. From experiments on cat motor cortex, Chen et al. (1996) found four distinguishable cell types, called regular spiking, burst firing, fast spiking and narrow spiking. Focussing attention on the first and third of these, corresponding to pyramidal cells and stellate cells, respectively, their time constants (means) were 12.2 ms and 4.8 ms and their apparent spike threshold depolarizations were 24 mV and 17.9 mV. The first spike frequencies (reciprocals of the times to elicit the first spike) for the regular spiking cells were between 30 Hz and 150 Hz for input currents between 0.3 nA and 0.9 nA, corresponding to values of $E[T_1]$ between 6.7 ms and 100 ms. For the stellate cells, currents between 0.8 nA and 2.2 nA gave first spike frequencies were between 20 Hz and 400 Hz, corresponding to values of $E[T_1]$ between 2.5 ms and 50 ms.

A rough estimate may be made of the currents which flow in pyramidal cells during synaptic excitation. Us-

ing the data of Chen et al. (1996) and the anatomical data from Megias et al. (2001) and assuming an epsp of amplitude 5 mV, input of 4500 epsp's per second is required to give a current of about 6 μ A per square cm which is about the threshold for repetitive firing in the standard HH model. Given that there are about 10,000 excitatory synapses on such cells, these figures seem reasonable for a phenomenological approach to cortical cells. The present calculations determine the moments of the first spike elicited from rest in the presence of random synaptic input. These calculations may be extended to include a random initial state (Lansky and Smith, 1989). Examples in the physiological range were $E[T_1] = 49.3$ ms (500 trials) with $\mu = 2.54$ and $\sigma = 1.61$ and $E[T_1] = 76.5$ ms (500 trials) with $\mu = 1.09$ and $\sigma = 1.78$. A systematic investigation gave the follows below.

We examined pre-first spike trajectories for $V(t)$ in the complete 4-component Hodgkin–Huxley system as well as the corresponding trajectories for the 2-component approximation. These are obtained by integrating the system using a strong Euler method (Tuckwell and Walsh, 1983), the choice of method being vindicated by the agreement obtained between analytical and simulation results (see below). The standard set of parameters was employed. We now denote the voltage firing threshold (Kistler et al., 1997) by θ . As a general rule, the longer the time to reach threshold, the worse is the agreement between the 2-component model and the full 4-component model. For example, when the input parameters are $\mu = 4$ and $\sigma = 1$, the approach of V to $\theta = 15$ is very much slower in the 4-component process than in the 2-component process.

When $\mu = 6$ and $\sigma = 2$, the sample paths for the 2- and 4-component processes attain the threshold value at similar rates and when $\mu = 15$ and $\sigma = 5$, the approach of $V(t)$ to θ is almost identical in the 2- and 4-component processes.

3.1. Mean time to a spike

The above sample-path properties are confirmed by examination of the means of the times to first attain threshold. In order to make a more detailed comparison, the means were determined by simulation for wide

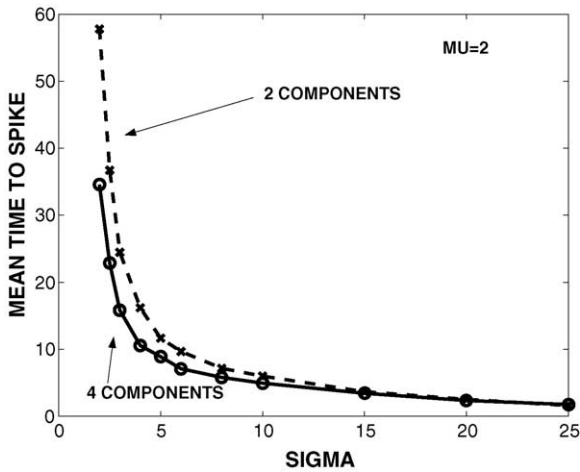


Fig. 1. Showing how the mean time to a spike, in ms, depends on σ for $\mu = 2 < \mu_c$ for the 4- and 2-component systems.

ranges of the values of μ and σ . Values of μ employed were well below, near or well above the critical value of $\mu = 4.15$ below which no spikes are elicited even for an indefinitely applied deterministic input current with that value of μ . We show in Figs. 1–3 results for a subthreshold $\mu = 2$, just above threshold $\mu = 5$ and a value well above threshold, $\mu = 10$ at various values of σ . The mean time to spike is plotted against the input noise standard deviation parameter σ for $\mu = 2$ in Fig. 1 and for $\mu = 5$ and 10 in Fig. 2. Results are shown in all figures for the 4-component model and the

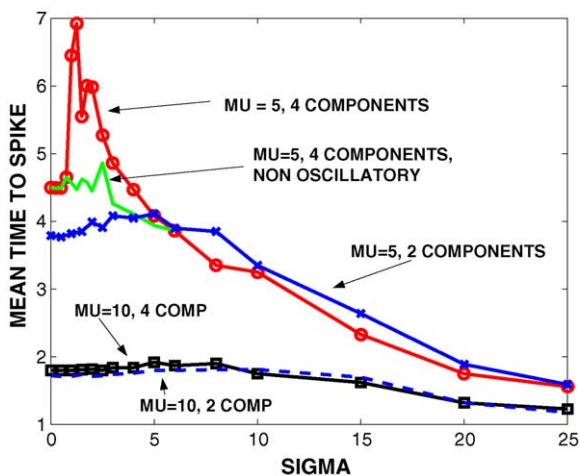


Fig. 2. Showing how the mean time to a spike, in ms, depends on σ for $\mu = 5$ and 10. For the explanation of the various curves, see text.

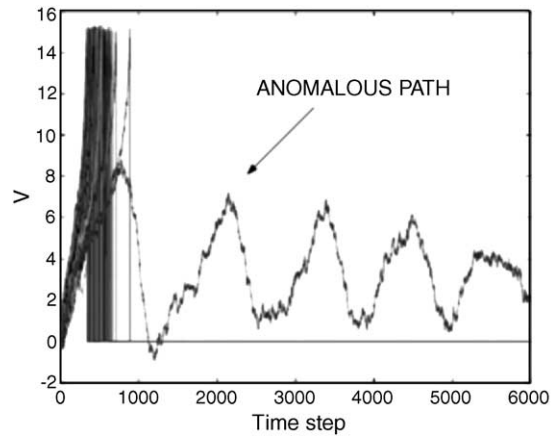


Fig. 3. A set of sample paths for V with $\mu = 5$ and $\sigma = 0.75$. Here nearly all paths go almost directly to threshold, except one anomalous path which spends a very long time wandering back and forth below threshold. For further details, see text.

2-component approximation. In Fig. 1, where $\mu = 2$, this agreement is good for $\sigma < \approx 8$, whereas for larger σ the value of $E[T_1]$ is considerably less than $E[\bar{T}_1]$. Agreement between the 4- and 2-component models is generally better the smaller the value of the time to spike.

In Fig. 2, where $\mu = 5$, agreement between $E[T_1]$ and $E[\bar{T}_1]$ is excellent for $\sigma > \approx 5$. The expected time to a spike in the full HH system displays a pronounced peak at about $\sigma = 1$. Note that the 2-component process slightly overestimates the expected firing time for large σ but underestimates it for $\sigma < \text{about } 5$. At small σ , being values less than 0.5, the paths show little departure from deterministic and most go more or less directly to threshold.

For larger σ (0.75) a new kind of path appears—one which may wander around at subthreshold values for a very long time. A set of results where this occurred is seen in Fig. 3 where $\mu = 5$ and $\sigma = 0.75$. There is shown one anomalous very long oscillatory path alongside 156 paths which went fairly directly to threshold. For various σ the proportion of such paths was examined. At $\sigma = 0.25$ and 0.5 there were no such paths in over 1000. When $\sigma = 0.75$, there were one or two in a thousand, but their effect on the mean (and higher moments) is large. The paths seem anomalous but they cannot be discarded. When they are discarded, the results shown by the green curve, labelled “non-oscillatory”, are obtained. By $\sigma = 1.25$ the proportion

of these paths, which we call “oscillatory” (meaning they wander back and forth between below threshold and more hyperpolarized states), has grown to about 2%. These effects were checked at various time step sizes to ensure they were not an artifact.

At $\sigma = 1.75$ the proportion of these very erratic paths has grown to about 6% and it continues to increase so that at $\sigma = 6$ and beyond such paths dominate. The proportion of almost direct paths steadily declines so there is a change in character of the underlying random process. Eventually nearly every path has an erratic and/or oscillatory character so that nearly all paths get to threshold at about the same time. The peak in the mean time to spike at around $\sigma = 2$ is due to the appearance of some extremely long paths amidst a majority of more direct ones. These results were obtained on the basis of a few thousand trials. It is possible that if the number of trials was greatly increased (to a million or so), the peak would be smoothed out. Also shown in Fig. 2 are the values of $E[T_1]$ and $E[\bar{T}_1]$ for $\mu = 10$. Here the 2- and 4-component models give practically the same result for all values of σ used. All observed paths were direct for $\sigma < \approx 6$ and for larger values of σ , as large as 25, there were hardly any erratic and/or oscillatory paths. Thus, there are a different number of regimes depending on the magnitude of μ relative to μ_c : one when μ is small and when μ is large; but three when μ is close to and above μ_c . Similar findings were reported on distributions of interspike intervals by Tiesinga et al. (2000).

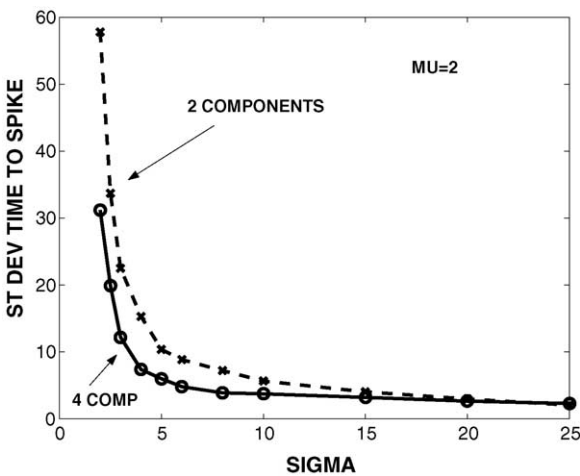


Fig. 4. Standard deviation of time to spike versus σ for $\mu = 2 < \mu_c$.

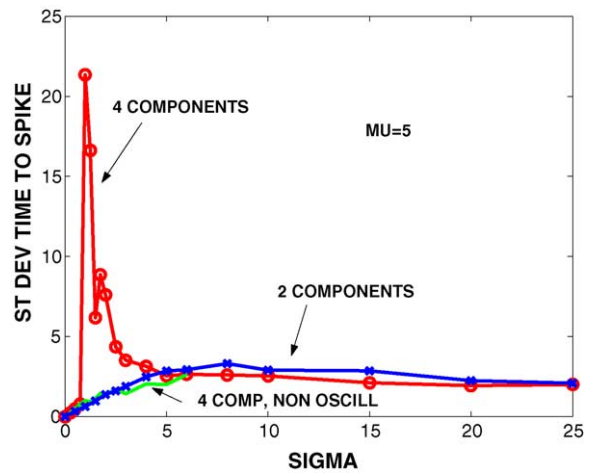


Fig. 5. Standard deviation of time to spike versus σ for $\mu = 5 > \mu_c$.

3.2. Standard deviation of time to a spike

In Figs. 4–6 we show the standard deviations of the time to spike as functions of σ for various μ , these results corresponding to the means shown in Figs. 1 and 2. In Fig. 4, where the value of $\mu = 2$ is well below the deterministic threshold current value, it can be seen that the results for the standard deviations mimic very closely the corresponding results for the mean. However, in the case $\mu = 5$ (Fig. 5), a very pronounced peak occurs around $\sigma = 1.5$ for the standard deviation as a function of σ in the full 4-component model. The peak

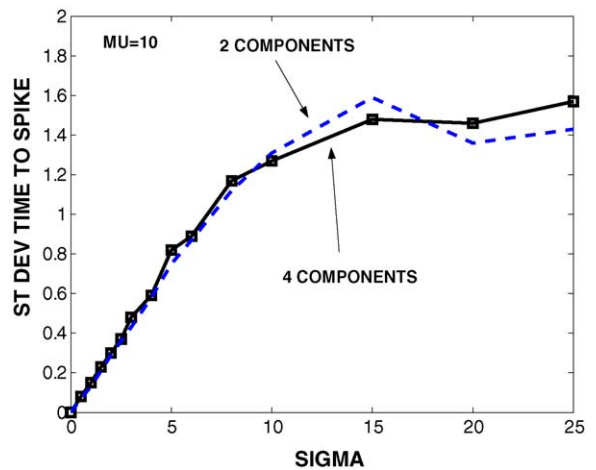


Fig. 6. Standard deviation of the time to spike versus noise amplitude for $\mu = 10$.

is apparently absent or indiscernible in the case of the 2-component model. Thus, in the HH neuron for just supra-threshold mean input currents, a small amount of noise in the input processes leads to a very large amount of uncertainty in the time to a spike—the coefficient of variation of the time to a spike is about 2.5 at the maximum. In Fig. 6 are shown the results for $\mu = 10$. Here the 2- and 4-component standard deviations are practically indistinguishable for all values of σ considered.

3.3. Coefficient of variation (CV) of time to a spike

In Figs. 7–9 is shown the dependence of the CV of the time to spike on σ for various μ . The results in Fig. 7 for $\mu = 2$ show a CV declining from $\sigma = 2$ to about 8, followed by an increase as $\sigma \rightarrow \infty$. In Fig. 8, where $\mu = 5$, a very pronounced maximum occurs for the HH model for values of σ between about 1 and 2, but is absent in the 2-component approximation. In all cases, both for the HH system and the 2-component approximation, and regardless of the value of μ , the CV tends to about 1.3 as $\sigma \rightarrow \infty$ in the range considered.

3.4. Analytical and other results for the mean

The equations for the mean time to threshold from rest in the 2-component approximation have been solved analytically using perturbation techniques

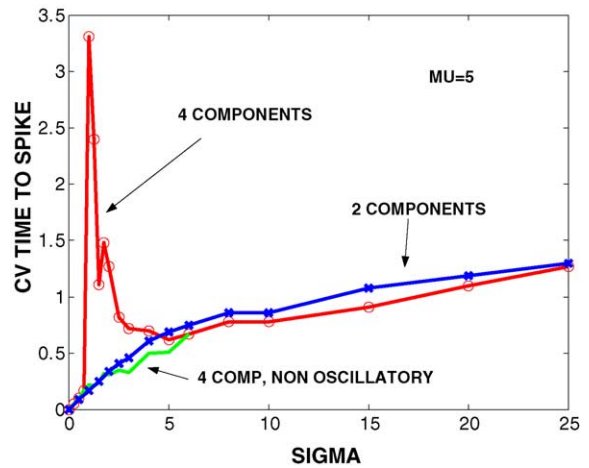


Fig. 8. Coefficient of variation of the time to spike against σ for $\mu = 5$.

which are presented elsewhere (Tuckwell and Wan, 2004). Such results are a useful check on those obtained by simulation. For example, with $\sigma = 0$, $\mu = 5$, the mean time to spike by simulation was 3.79 (four components) whereas analytical methods gave 3.76 (two components). Also, when $\sigma = 10$ and $\mu = 5$, the analytical method gave a mean of 3.38 whereas simulation gave 3.35. A 1-component approximation in which h, m, n are fixed was also investigated, as analytical methods are then simplest. However, results for the first two moments for all values of μ were extremely inac-

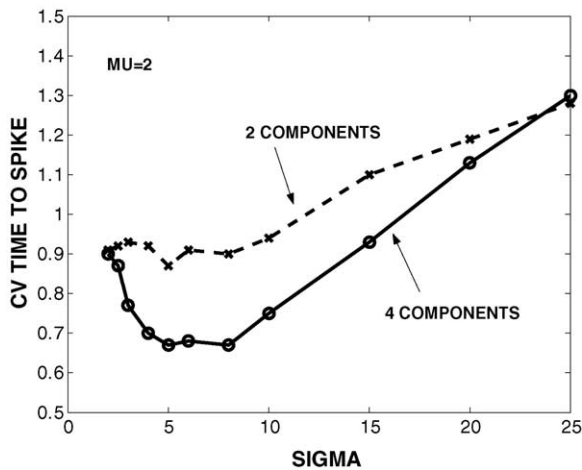


Fig. 7. Coefficient of variation of the time to spike against σ for $\mu = 2$.

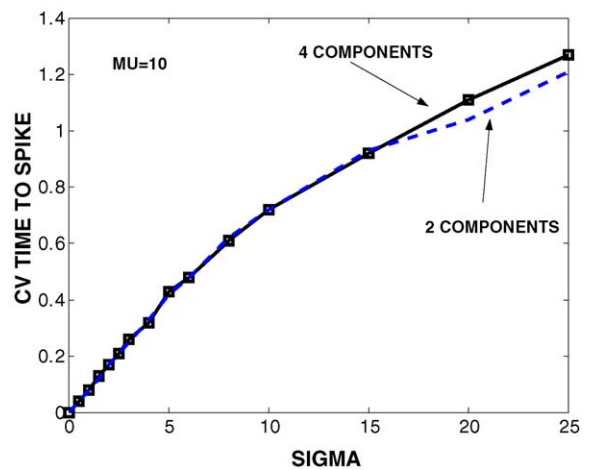


Fig. 9. Coefficient of variation of the time to spike against σ for $\mu = 10$.

curate until σ was as large as 15–20, where the time to threshold is practically independent of the neuronal dynamics.

4. Determination of the interspike interval

The above theory applies to the time taken to the appearance of the first spike, elicited from rest, which is a well defined random variable because the initial conditions may be stated precisely, possibly with a distribution of values. To obtain the interspike interval (ISI), assuming again the input processes are temporally homogeneous, we may proceed by an approximate method outlined below. However, some observations on spike trains generated by space-clamped Hodgkin–Huxley and other similar conductance based model neurons are in order.

In renewal models such as (leaky) integrate and fire, the neuron depolarization is reset after a spike, possibly to a random value. In contrast, in the HH stochastic model, there is no reset and it is fairly safe to say that no two spikes have the same trajectory in (V, n, m, h) -space. We examined two spike trains (see Fig. 10) with the same initial conditions, same dynamical system parameters and the same input parameters for the mean and standard deviation of the stimulus. The standard pa-

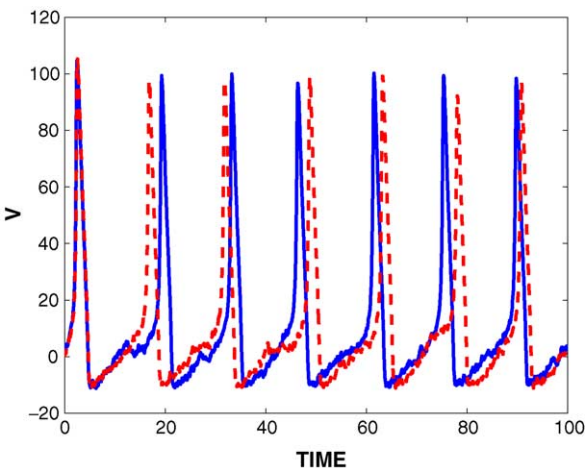


Fig. 10. Two Hodgkin–Huxley spike trains, (ordinates in mV), with the same parameters and initial conditions. These are two distinct computer generated solutions of the stochastic Eq. (1), assuming a neuron initially at rest. Different trajectories reflect purely random differences in input currents, representing synaptic inputs.

rameters were used to generate these trains with $\mu = 10$ and $\sigma = 2$.

In a way that contradicts the findings of reliability in the presence of stochasticity, although the first spikes of each train occur at about the same time, one train sometimes leads and sometimes lags the other train. Members of each sequence of interspike intervals are far from being independent and the most meaningful observable is not the ISI but the entire vector of spike times $T = (T_1, T_2, \dots, T_n)$, or more precisely the whole random trajectory $\{(V(t), n(t), m(t), h(t)), 0 \leq t \leq t_{\text{final}}\}$, because a sample path for the noise generates such an entire sequence rather than a collection of independent ISIs. There is also a problem in defining an ISI: the method sometimes employed in taking the time interval between successive crossings of resting level, or any other fixed voltage, is not completely satisfactory since it is feasible that V could swing back and forth across resting value without any accompanying spikes.

These aspects are highlighted by considering the probability density of $V(t)$, the first component of the 4-component process

$$\{(V(t), n(t), m(t), h(t)), 0 \leq t \leq t_{\text{final}}\}.$$

This is the solution of the Kolmogorov equation for the transition probability density with the three variables n, m , and h integrated out. For the same set of parameter values employed to generate the spike trains referred to in the previous paragraph, this probability density is shown in Fig. 11 at the nine different times indicated on top of each histogram, these data being obtained from 500 trials. The initial density is a delta function which by $t = 1$ has spread to a narrow gaussian-like density. By $t = 1.8$, just before the mean time of arrival of the first spike there is a small mass of probability at about 90 mV which subsequently grows quite large by $t = 3.00$.

The distribution of probability mass recedes from high values of V and accumulates strongly at hyperpolarized values by $t = 6$. At times just before the second spike, such as at $t = 16$, again a small amount of probability appears at and above 90 mV, indicating that the peak of a spike may occur at such times. However, the probability distribution subsequently becomes smeared out over the whole range of possible values of V . This means that all values of V are about equally likely and it is not possible to pick out any particular time at which

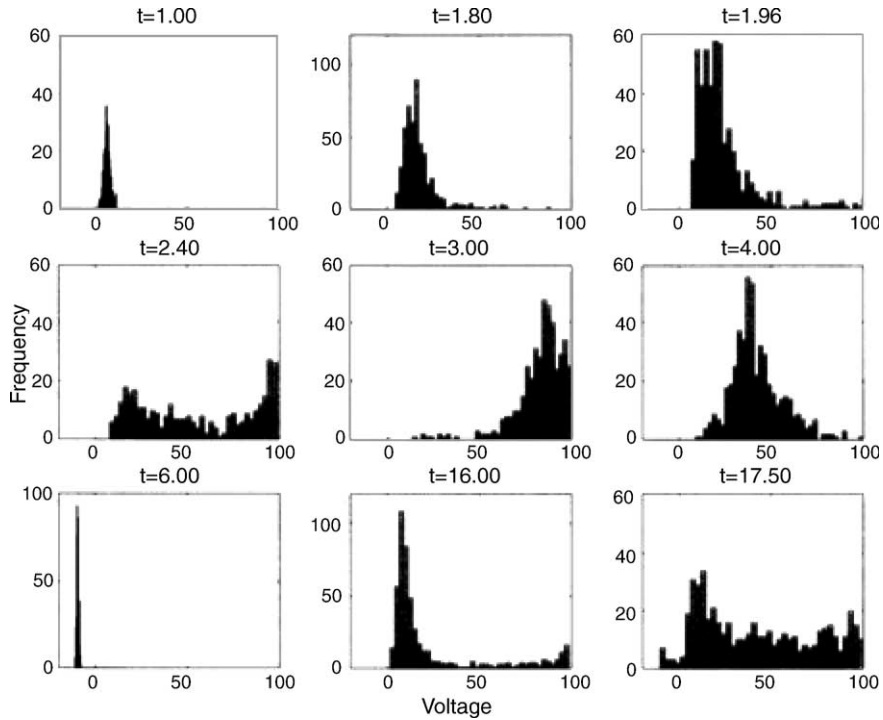


Fig. 11. Histograms representing the probability distribution of the depolarization in the stochastic Hodgkin–Huxley model at various times as indicated at the top of each frame. Here and in the next figure the standard parameters are employed and the current input parameters are $\mu = 10$ and $\sigma = 2$.

a second and subsequent spike has a particularly large chance of occurring. As time increases, the probability distribution of V becomes almost uniform and it is apparent that asking for the (random) time to a spike, given that there was a spike at a particular time, t_0 , say, is only possible if the values of the remaining three variables n , m , and h are known at t_0 . The problem would be compounded considerably if one were to consider the spatial distribution of potential throughout the soma and dendrites.

However, we may sometimes use the following approximate method to estimate the time to the next spike when the noise is not too large and the firing rate is not too high. With input values the same as previously in this section, the left-hand top corner of Fig. 12 shows the the distribution of the value of the minimum of V , called V_{\min} , which occurs at hyperpolarized values just after a spike, before the upward excursion to the next threshold crossing. The corresponding values of the remaining three components are designated n^* , m^* , and h^* and their distributions are also shown in Fig. 12.

Note that these histograms are obtained from several hundred spikes and are quite distinct from those of Fig. 11 where the potential distribution was given as a function of time. All four distributions are relatively tight so that it is reasonable to use their means, \bar{V}_{\min} , \bar{n}^* , \bar{m}^* , and \bar{h}^* , as initial conditions in the following way. Examination of typical spikes shows that we may decompose the k -th ISI into a random part and a deterministic part:

$$ISI_k = T(V_{\min,k} \rightarrow v_\theta) + t(v_\theta \rightarrow V_{\min,k+1}).$$

The first part is the random time for V to go from the k th minimum after the k th spike to a threshold value v_θ and the second part is the (practically) deterministic time for the voltage to swing from threshold to peak depolarization and then to its $(k + 1)$ th minimum, which may occur at hyperpolarized values or sometimes at depolarized values if the cell is firing rapidly. The same theory employed to find the random time to the first spike may be applied to determine $T(V_{\min} \rightarrow v_\theta)$, us-

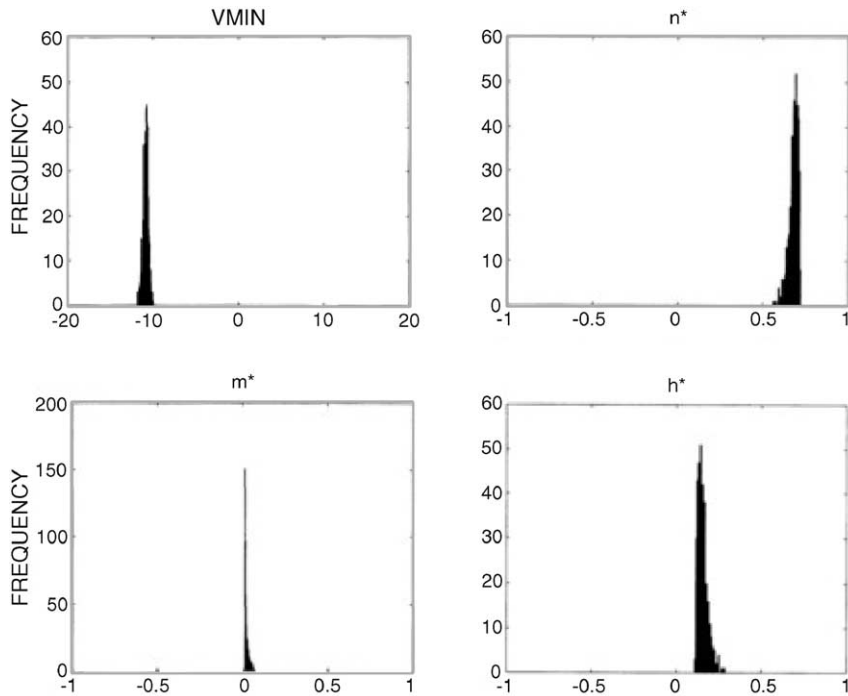


Fig. 12. The probability distribution of the minimum voltage (depolarization in mV) after a spike is shown in the top left frame and the distributions of the corresponding values of the remaining variables n , m , and h are shown in the remaining frames.

ing $\bar{P} = (\bar{V}_{\min}, \bar{n}^*, \bar{m}^*, \bar{h}^*)$ or the corresponding deterministic ($\sigma = 0$) point $P = (V_{\min}, n^*, m^*, h^*)$ as an initial point. This was done for the input parameters $\mu = 10$ and $\sigma = 2$, yielding an estimate of the mean interspike time as 14.8 ms, when the deterministic point V is the initial value and 14.7 ms when the mean point \bar{P} is used. These results compare favorably with the mean value of 15.1 ms from the simulated spike train (200 observations).

5. Discussion and conclusions

After the formulation of systems of stochastic differential equations for the space-clamped HH model (Tuckwell, 1986), there were relatively few theoretical investigations of the theory of firing properties, probably because most available computing facilities were still inadequate. In this paper an analytical approach has been outlined, based on the threshold voltage concept, (Kistler et al., 1997) to finding the statistics of the time to first spike. The latter is an experimentally observed

quantity (Chen et al., 1996) and the present model applies to such experimental observations because there may be intrinsic noise due to random synaptic bombardment, which may be approximated by a non-zero mean Gaussian white noise current.

For the first spike elicited from a rest state, one may employ Markov process theory to obtain statistical properties, including moments and probability distribution. Analytical methods of solution of the equations are presented elsewhere (Tuckwell and Wan, 2004). Extensive simulations were performed for the HH-system and the 2- and 1-component approximations with a view to ascertaining where the approximations are accurate. We focussed on the first two moments of the time to a spike (the random variable T_1 for the full HH system) and found peaks in the mean and standard deviation of T_1 at small values of the input noise parameter σ when the mean current μ was near threshold in the absence of noise. Pronounced peaks were found in the moments and coefficient of variation of T_1 as a function of σ for certain values of μ . There are a different number of regimes depending on the magnitude

of μ relative to μ_c : one when μ is small and when μ is large; but three when μ is close to and above μ_c . The sample paths in the 2-component approximation were very close to those of the HH system when the time to spike is small ($<$ about 5 ms).

We also considered the more difficult problem of estimating the ISI. We emphasized that traditional concepts associated with renewal models do not apply to conductance-based models such as HH. Although the threshold voltage concept is not adequate in general for determining the ISI, we have applied a decomposition of the ISI into random and quasi-deterministic components to successfully estimate the mean ISI for certain parameter values.

Acknowledgment

The author appreciates the hospitality of Professor Ruth J. Williams at UCSD Mathematics.

Appendix A. Hodgkin–Huxley coefficients

$$\alpha_n(V) = \frac{10 - V}{100[e^{(10-V)/10} - 1]}$$

$$\beta_n(V) = \frac{1}{8} e^{-V/80}$$

$$\alpha_m(V) = \frac{25 - V}{10[e^{(25-V)/10} - 1]}$$

$$\beta_m(V) = 4 e^{-V/18}$$

$$\alpha_h(V) = \frac{7}{100} e^{-V/20}$$

$$\beta_h(V) = \frac{1}{e^{(30-V)/10} + 1}$$

References

- Burns, B.D., Webb, A.C., 1976. The spontaneous activity of neurones in the cat's cerebral cortex. *Proc. R. Soc. Lond. B* 194, 211–223.
- Chen, W., Zhang, J.-J., Hu, G.-Y., Wu, C.-P., 1996. Electrophysiological and morphological properties of pyramidal and nonpyramidal neurons in the cat motor cortex in vitro. *Neuroscience* 73, 39–55.
- deCharms, R.C., Zador, A., 2000. Neural representation and the cortical code. *Ann. Rev. Neurosci.* 23, 613–647.
- Destexhe, A., Pare, D., 2000. A combined computational and intracellular study of correlated synaptic bombardment in neocortical pyramidal neurons in vivo. *Neurocomputing* 32–33, 113–119.
- Feng, J., Li, G., 2001. Integrate-and-fire and Hodgkin–Huxley models with current inputs. *J. Phys. A* 34, 1649–1664.
- Fox, R.F., Lu, Y., 1994. Emergent collective behavior in large numbers of globally coupled independently stochastic ion channels. *Phys. Rev. E* 49, 3421–3431.
- Gluss, B., 1967. A model for neuron firing with exponential decay of potential resulting in diffusion equations for probability density. *Bull. Math. Biophys.* 29, 233–43.
- Hodgkin, A.L., Huxley, A.F., 1952. A quantitative description of membrane current and its application to conduction and excitation in nerve. *J. Physiol.* 117, 500–544.
- Kistler, W.M., Gerstner, W., van Hemmen, J.L., 1997. Reduction of the Hodgkin–Huxley equations to a single-variable threshold model. *Neural Comput.* 9, 1015–1045.
- Kreiter, A.K., Singer, W., 1996. Stimulus-dependent synchronization of neuronal responses in the visual cortex of the awake macaque monkey. *J. Neurosci.* 16, 2381–2396.
- Lansky, P., Smith, C.E., 1989. The effect of a random initial value in neural 1st passage time models. *Math. Biosci.* 93, 191–215.
- Lee, S.-G., Kim, S., 1999. Parameter dependence of stochastic resonance in the stochastic Hodgkin–Huxley neuron. *Phys. Rev. E* 60, 826–830.
- Mainen, Z.F., Joerges, J., Huguenard, J.R., Sejnowski, T.J., 1995. A model of spike initiation in neocortical pyramidal neurons. *Neuron* 15, 1427–1439.
- Manwani, A., Steinmetz, P.N., Koch, C., 2002. The impact of spike timing variability on the signal-encoding performance of neural spiking models. *Neural Comput.* 14, 347–367.
- Meffin, H., Burkitt, A.N., Grayden, D.B., 2004. An analytical model for the ‘Large, fluctuating synaptic conductance state’ typical of neocortical neurons in vivo. *J. Comp. Neurosci.* 16, 159–175.
- Megias, M., Emri, Z.S., Freund, T.F., Gulyas, A.I., 2001. Total number and distribution of inhibitory and excitatory synapses on hippocampal CA1 pyramidal cells. *Neuroscience* 102, 527–540.
- Pare, D., Lang, E.J., Destexhe, A., 1998. Inhibitory control of somadendritic interactions underlying action potentials in neocortical pyramidal neurons in vivo: an intracellular and computational study. *Neuroscience* 84, 377–402.
- Plesser, H.E., Gerstner, W., 2000. Noise in integrate-and-fire neurons: from stochastic inputs to escape rates. *Neural Comput.* 12, 367–384.
- Rinzel, J., 1978. Repetitive activity in nerve. *Fed. Proc.* 37, 2793–2802.
- Schmid, G., Goychuk, I., Hanggi, P., 2004. Effect of channel block on the spiking activity of excitable membranes in a stochastic Hodgkin–Huxley model. *Phys. Biol.* 1, 61–66.
- Skaugen, E., Walløe, L., 1979. Firing behavior in a stochastic nerve membrane model based upon the Hodgkin–Huxley equations. *Acta Physiol. Scand.* 107, 343–363.

- Stein, R.B., 1967. The frequency of nerve action potentials generated by applied currents. *Proc. R. Soc. Lond. B* 167, 64–86.
- Steinmetz, P.N., Manwani, A., Koch, C., 2001. Variability and coding efficiency of noisy neural spike encoders. *BioSystems* 62, 87–97.
- Steinmetz, P., Manwani, A., Koch, C., London, M., Segev, I., 2000. Subthreshold voltage noise due to channel fluctuations in active neuronal membranes. *J. Comput. Neurosci.* 9, 133–148.
- Steriade, M., Wyzinski, P., Apostol, V., 1973. Differential synaptic reactivity of simple and complex pyramidal tract neurons at various levels of vigilance. *Exp. Brain Res.* 17, 87–110.
- Troyer, T.W., Miller, K.D., 1998. Physiological gain leads to high ISI variability in a simple model of a cortical regular spiking cell. In: Abbott, L., Sejnowski, T.J. (Eds.), *Neural Codes and Distributed Representations: Foundations of Neural Computation*. MIT, Cambridge, MA, pp. 187–308.
- Tiesinga, P.H.E., Jose, J.V., Sejnowski, T.J., 2000. Comparison of current-driven and conductance-driven neocortical model neurons with Hodgkin–Huxley voltage-gated channels. *Phys. Rev. E* 62, 8413–19.
- Tuckwell, H.C., 1979. Synaptic transmission in a model for stochastic neural activity. *J. Theor. Biol.* 77, 65–81.
- Tuckwell, H.C., 1986. Stochastic equations for nerve membrane potential. *J. Theor. Neurobiol.* 5, 87–99.
- Tuckwell, H.C., 1989. *Stochastic Processes in the Neurosciences*. SIAM, Philadelphia.
- Tuckwell, H.C., Rodriguez, R., 1998. Analytical and simulation results for stochastic Fitzhugh–Nagumo neurons and neural networks. *J. Comput. Neurosci.* 5, 91–113.
- Tuckwell, H.C., Wan, F.Y.M., Rodriguez, R., 2002. Analytical determination of firing times in stochastic nonlinear neural models. *Neurocomputing* 48, 1003–1007.
- Tuckwell, H.C., Walsh, J.B., 1983. Random currents through nerve membranes. *Biol. Cybern.* 49, 99–110.
- Tuckwell, H.C., Wan, F.Y.M., 2004. Time to spike in stochastic Hodgkin–Huxley system. *Physica A* (in press).
- Yu, X., Lewis, E.R., 1989. Studies with spike initiators: linearization by noise allows continuous signal modulation in neural networks. *IEEE Trans. Biomed. Eng.* 36, 36–43.